NONEQUILIBRIUM AND RAREFACTION EFFECTS IN THE HYPERSONIC MULTICOMPONENT VISCOUS SHOCK LAYERS

Vladimir V. Riabov
Rivier College, Nashua, New Hampshire 03060, USA

Abstract

The effects of rarefaction and nonequilibrium processes on hypersonic rarefied-gas flows over blunt bodies have been studied by the Direct Simulation Monte-Carlo technique (DSMC) and by solving the full Navier-Stokes equations and the equations of a thin viscous shock layer (TVSL) under the conditions of wind-tunnel experiments and hypersonic-vehicle flights at altitudes from 60 to 110 km. The nonequilibrium, equilibrium and "frozen" flow regimes have been examined for various physical and chemical processes in air, including excitation of translational, rotational and vibrational degrees of molecular freedom, as well as dissociation, chemical reactions, and ionization in the layers near catalytic body surface. The influence of similarity parameters (Reynolds number, temperature factor, catalyticity parameters, and geometrical factors) on the flow structure near the blunt body and on its aerodynamic coefficients in hypersonic streams of dissociating air is studied. The analysis of the catalytically influenced zone of the flow near the surface demonstrates that in order to increase the accuracy of the determination of heat flux values, it is necessary to utilize more reliable information on transfer properties of multicomponent gas mixture and the constants of chemical reaction rates. The main characteristics of the catalytically influenced zone (its width, temperature, and concentrations of species on the external boundary of the zone) can be useful for development of new approximation methods of predicting the heat fluxes at catalytic surface materials of a vehicle.

The numerical results are in a good agreement with experimental data, which were obtained in wind tunnels at low and moderate Reynolds numbers from 1.49 to 5130, as well as STS flight data. It has been confirmed that the binary-scaling similitude law is satisfied for blunt bodies in the transition flow regime.

1 Introduction

Planetary exploration programs [1] stimulate new studies in hypersonic high-temperature gas dynamics and aerothermodynamics. The areas of aerodynamic heating and heat protecting techniques have brought renewed interests in the design of modern hypersonic vehicles [2-5].

To analyze the structure of the flows of a chemical nonequilibrium multicomponent gas (air) near a blunt body, one of the approximations of the Navier-Stokes equations has been used, namely, a model of a thin viscous shock layer (TVSL) developed by Cheng [2, 6], Moss [7], Miner and Lewis [8], Anderson [9], and Gusev et al. [10]. Using this model of the TVSL with the generalized Rankine-Hugoniot conditions [10, 11], a study of streamlining the blunt bodies (with spherical and cylindrical nose shapes) by hypersonic air-flow under re-entry conditions at the altitudes from 110 to 60 km were conducted.

The influence of different approximation models of the mass diffusion flux, heat flux and the values of the chemical reaction rates has been studied. The results of the calculations of the flow characteristics in the viscous shock layer around blunt bodies are obtained for different degree of catalytic activity on the vehicle surface. Studies have been conducted on

the characteristics of the catalytically influenced zone of the flow near the catalytic surface of the body. It is the catalytic properties of the body surface, as well as diffusion gas characteristics, that define the features of this specific zone. The present results are the development of the research conducted by Gusev et al. [10] and Provotorov and Riabov [11-16].

Calculations of the Stanton number in the stagnation point of the spherical one-meter-radius body, with dependency on the Reynolds number Re_{of} along the Space Shuttle trajectory [17], are in good agreement with flight data [24, 37]. The results are compared with the solutions of full viscous shock-layer (FVSL) and high-order viscous shock-layer (HVSL) (see Refs. 18-22). It has been shown that both a body and a shock slip model are required with the VSL calculations to receive physically meaningful results at higher altitudes (in the range of 90 to 110 km). A detailed comparison of the results from various prediction methods (including numerical solutions of the full Navier-Stokes equations [23] and the Direct Simulation Monte Carlo (DSMC) technique [24-26]) has been provided as well.

2 Approximation of a Thin Viscous Shock Layer (TVSL)

A formulation of the corresponding boundary-value problem in terms of the TVSL, as well as the system of differential equations and boundary conditions has been developed by many researchers [6-16]. The TVSL equations are found from asymptotic analysis of the Navier-Stokes equations [6, 11] at $\varepsilon \to 0$, $Re_{of} \to \infty$, and $\sigma = (\varepsilon Re_{of}) = $ const, where $Re_{of} = \rho_\infty U_\infty R / \mu(T_{of})$ is Reynolds number, $\varepsilon = (\gamma-1)/(2\gamma)$, γ is a specific heat ratio. In the case of nonequilibrium hypersonic flow near a body, the TVSL equations are as following [11-14]:

$$\partial(g_2\rho u)/\partial x + \partial(g_1 g_2 \rho v)/\partial y = 0 \qquad (1)$$

$$\rho(ug_1^{-1}\partial u/\partial x + v\partial u/\partial y) = -\varepsilon g_1^{-1}dp_w/dx \\ +\sigma\partial(\mu\partial u/\partial y)/\partial y \qquad (2)$$

$$\partial p/\partial y = K\rho u^2 \qquad (3)$$

$$\rho(ug_1^{-1}\partial w/\partial x + v\partial w/\partial y) \\ =\sigma\partial(\mu\partial w/\partial y)/\partial y \qquad (4)$$

$$\rho(ug_1^{-1}\partial H/\partial x + v\partial H/\partial y) = -\partial q/\partial y \\ +2\sigma\partial(\mu u\partial u/\partial y)/\partial y+2\sigma\partial(\mu w\partial w/\partial y)/\partial y \qquad (5)$$

$$\rho(ug_1^{-1}\partial A_l/\partial x + v\partial A_l/\partial y) = -\partial J_l/\partial y, \\ l=1, 2, ..., N_{el}-1 \qquad (6)$$

$$\rho(ug_1^{-1}\partial \alpha_i/\partial x + v\partial \alpha_i/\partial y) = -\partial j_i/\partial y+\omega_i, \\ i= N_{el}, ..., N-1 \qquad (7)$$

$$\Sigma\alpha_k = 1, k = 1, 2, ..., N \qquad (8)$$

$$p= \rho R_g T \qquad (9)$$

Here xL and $yL\varepsilon$ are surface coordinates; uU_∞, vU_∞/ε, and wU_∞ are tangential, normal and binormal components of velocity vector; $\rho\rho_\infty/\varepsilon$ is density; $pp_\infty U_\infty^2$ - pressure; $\alpha_i = \rho_i/\rho_\infty$ - mass concentration of i-species; $\omega_i\rho_\infty U_\infty/(\varepsilon L)$ - generation rate of i-species; A_l - mass concentration of l-element; g_1 and g_2 are Lame's coefficients; p_w - pressure on the body surface. Formulas for viscosity μ, total enthalpy H, heat flux q, mass fluxes of species (j_i) and elements (J_l), specific heats, and species rates ω_i can be found in Refs. 11-14, and 27. The method of calculating transport coefficients of atmospheric dissociating gases has been described in Ref. 28.

The conditions of adhesion and nonpenetration are assumed to be specified at the surface of the body, as are the conditions of equilibrium-radiation heat exchange and mass component balances with consideration of various catalytic properties of the surface material. The generalized Rankine-Hugoniot conditions [11-14, 27] are assumed to be satisfied at the external boundary of the thin viscous shock layer:

$$\sin\chi\cos\varphi(\cos\chi\cos\varphi - u) = \sigma\mu\partial u/\partial y \qquad (10)$$

$$\rho v = - \sin\chi\cos\varphi \qquad (11)$$

$$\sin\chi\cos\varphi(\sin\varphi - w) = \sigma\mu\partial w/\partial y \qquad (12)$$

$$p = \sin^2\chi\cos^2\varphi \qquad (13)$$

$$\sin\chi\cos\varphi(H_\infty - H) = -q \\ +2\sigma\mu(u\partial u/\partial y + w\partial w/\partial y) \qquad (14)$$

$$\sin\chi\cos\varphi(A_{l\infty} - A_l) = -J_l \qquad (15)$$

$$\sin\chi\cos\varphi(\alpha_{i\infty} - \alpha_i) = -j_i \qquad (16)$$

Here χ is a swept angle and φ is a shock incident angle that is the generatrix angle in the TVSL approximation [14].

3 Numerical Method and Some Results

The numerical procedure of Provotorov and Riabov [11-15] was used for the solution of nonlinear partially differential equations (1)-(7) with a small parameter at the higher derivatives. The equation terms have been approximated by using the two-point second-order Keller's scheme [29, 30]. The results have been obtained in the whole range of chemical reaction rates up to the values near equilibrium. The iteration process permits one to obtain a rapid convergence of the second order towards the solution. This property of the numerical algorithm is especially significant when the influence of the recombination processes on the flow structure is essential. In the present study, the number of iterations was below six.
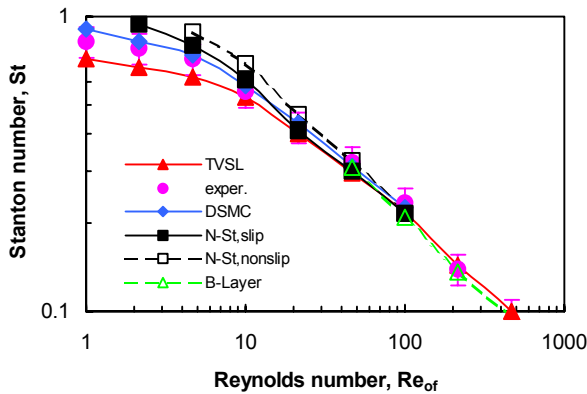

Fig 1. Stanton numbers *St* for a sphere vs. Reynolds numbers *Re*ₒf for different medium models at various wind-tunnel experimental conditions [16, 31-33].

The values of the Stanton numbers St at the stagnation point of a sphere were calculated under wind-tunnel conditions at various Reynolds numbers $Re_{of} = \rho_\infty U_\infty R/\mu(T_{of})$, Mach number $M_\infty = 15$, and temperature factor $t_w = 0.15$. The comparison between the results from the TVSL (triangles) model and the solutions of the full system of the Navier-Stokes equations with slip (filled squares) and non-slip (empty squares) boundary conditions is shown in Fig. 1. The results correlate well with experimental data [16, 31-33] (circles) and numerical data obtained by the DSMC method [26] (diamonds).
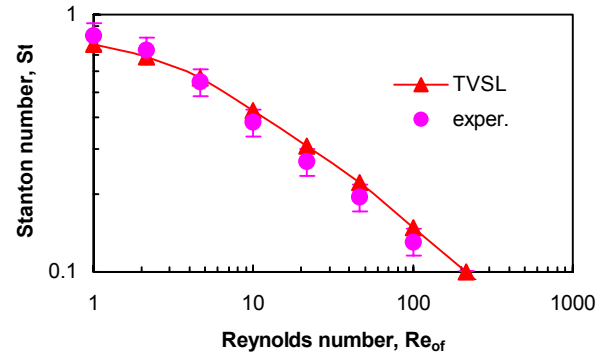

Fig 2. Stanton numbers *St* for a cylinder vs. Reynolds numbers *Re*ₒf for different medium models at various wind-tunnel experimental conditions [16, 34, 35].

The results of the Stanton number St at the stagnation line of a cylinder were also calculated by the TVSL model (triangles) and shown in Fig. 2. The results correlate well with experimental data [16, 34, 35] (circles).
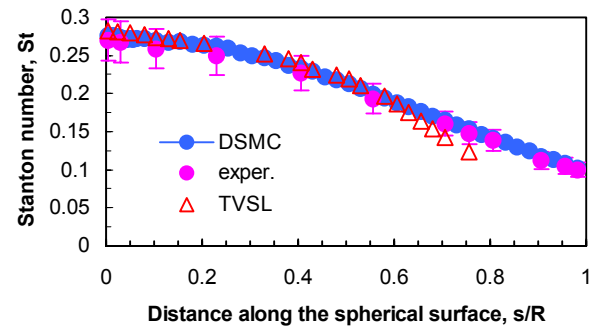

Fig 3. Stanton numbers *St* along the spherical surface coordinate *s/R* at *Re*ₒf = 46.38, *M*∞ = 6.5, *t*ʷ = 0.31. Experimental data from Refs. 16 and 36.

A comparison between the results from the TVSL model (triangles), experimental data [16, 36] (circles) and numerical data obtained by the

DSMC method [26] (diamonds) along the spherical surface is shown in Fig. 3. The parameters of upstream perfect gas flow were the following: $Re_{of} = 46.38$, $M_\infty = 6.5$, $t_w = 0.315$, and $\gamma = 1.4$.
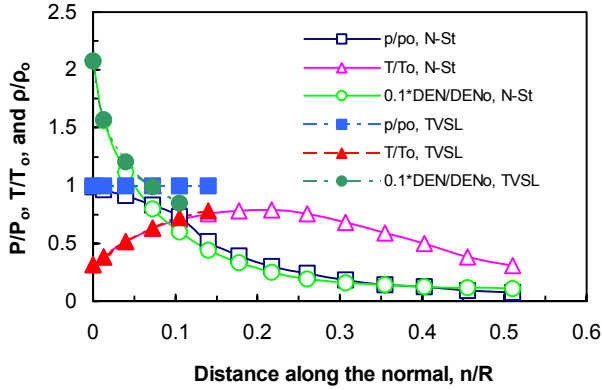

Fig. 4 Pressure, temperature and density along the normal on the critical line of a sphere at $Re_{of} = 7.33$, $M_\infty = 6.5$, and $t_w = 0.315$.

A comparison between the results obtained by the TVSL model (dashed lines) and the solutions of the full system of the Navier-Stokes equations with no slip boundary conditions (solid lines) is made and shown in Fig. 4. The parameters of upstream perfect gas flow were the following: $Re_{of} = 7.33$, $M_\infty = 6.5$, $t_w = 0.315$, $\gamma = 1.4$. The largest difference in the distributions of parameters calculated from the TVSL model at low Reynolds numbers Re_{of} was observed far away from the wall of the sphere where the condition, $p = const$, no longer holds along the central streamline. The agreement between the two sets of data on the distribution of parameters over the surface of the body itself is rather satisfactory (see also Ref. 10). All this indicates that it is possible to use the model of a thin viscous shock layer in studying the hypersonic flow over blunt bodies in the transition region at low Reynolds numbers Re_{of}.

3 Calculation Results

Calculations of the Stanton number $St = q/(\rho_\infty U_\infty (H_o - H_w))$ in the critical point of the spherical one-meter radius body, with dependency on the Reynolds number Re_{of} along the Space Shuttle trajectory [17, 24] (see Table 1), are shown in Fig. 5. The viscosity coefficient

μ is calculated at the stagnation temperature T_{of} and "frozen" upstream conditions [10].

Table 1. Values of the Reynolds number for a sphere (R=1m) along the Space Shuttle trajectory [17, 24]

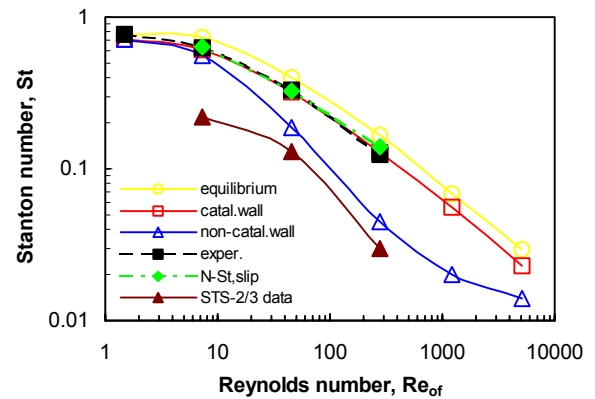| h, km	Re_{of}
110	1.49
100	6.97
90	47.3
80	230
70	1220
60	5130

Fig 5. Stanton numbers St vs. Reynolds numbers Re_{of} for a sphere of radius R=1m along the Space Shuttle trajectory and different medium models. Wind-tunnel experimental data from Refs. 16, 31-33; STS-2 and STS-3 data from Ref. 24.

The degree of catalytic activity of the body's surface material significantly influences the value of heat flux q. The greater the difference of the value q between the absolutely noncatalytic (empty triangles) and ideally catalytic (empty squares) surface indicated decreasing velocity with decreasing re-entry flight altitudes, h (or increasing Re_{of}). The direct relationship was noticed below the 80 km range ($Re_{of} = 230$). The values of heat flux under the flight conditions at this altitude differ by factor of three for various catalytic vehicle surfaces. These significant differences point to the nonequilibrium character of physical and chemical processes in the thin viscous shock layer under the considered conditions, which is confirmed by the STS-2 and STS-3 flight data [37] (filled triangles, Fig. 5).

The flight velocity U_∞ is one of the defining parameters of the flow around the

vehicle [14]. In the case of the flight altitude of $h = 80$ km with constant velocity $U_\infty = 7.9$ km/sec, a significant decrease of the Stanton number St is noticed between the noncatalytic surface and calculated value. At the altitude of $h = 67.5$ km this difference reaches 240%. At the same time, the degree of influence of this parameter in the case of ideally catalytic surfaces is insignificantly small [14].

A certain pattern in the values of q for the ideal catalytic surface material has been observed in a number of publications [7-24] at different flight conditions and different models of physical and chemical processes in the TVSL. The results of the calculations of the nonequilibrium layer near the catalytic surface at high level of accuracy correlate with the data [13] obtained for equilibrium viscous shock layer are show in Fig.5 (circles).

The degree of catalytic surface activity does not noticeably influence such values as pressure, thickness of the shock layer and coefficient of friction [10-15]. The research done in this study for altitudes of 60 - 110 km confirmed this conclusion.

The degree by which the nonequilibrium physical and chemical processes influenced the flow in the TVSL at small magnitudes of the Reynolds number $1 \leq Re_{of} \leq 49$ was analyzed by Gusev et al. [10] and Provotorov and Riabov [11, 12]. The results of the calculations for the conditions of the flight at higher Reynolds numbers (and lower altitudes) are displayed in Figs. 6-11.
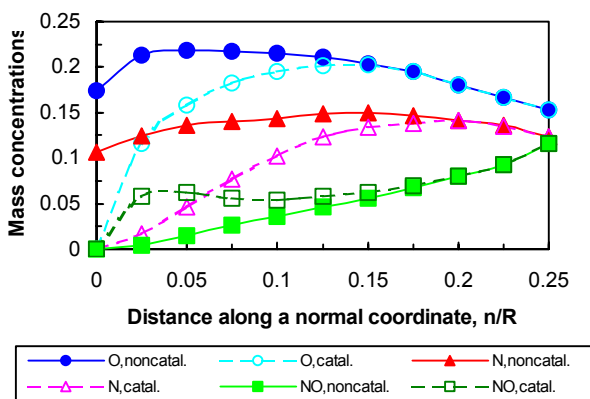
The distribution of the mass concentration of the air components $\alpha_i = \rho_i/\rho$ at the Reynolds number $Re_{of} = 230$ and the flight conditions at altitude $h = 80$ km is shown in Fig. 6. The degree of catalytic surface activity influences significantly the component distributions in the viscous shock layer. The specific measure of this influence is the width of the catalytically influenced zone d, which is characterized by the significant difference in the component distributions α_i for two extreme cases: ideally catalytic (dash lines) and absolutely noncatalytic (solid lines) surfaces. Thus, the flight conditions at these altitudes fully define the degree of dissociation of molecules O_2, NO, N_2, and concentrations of O and N atoms as well as the catalytically influenced zone d. As it was mentioned in the studies of Gusev et al. [10] and Provotorov and Riabov [11, 12], this influence was distributed through the whole thickness of the viscous shock layer, under the above mentioned conditions at $h = 90 - 110$ km.
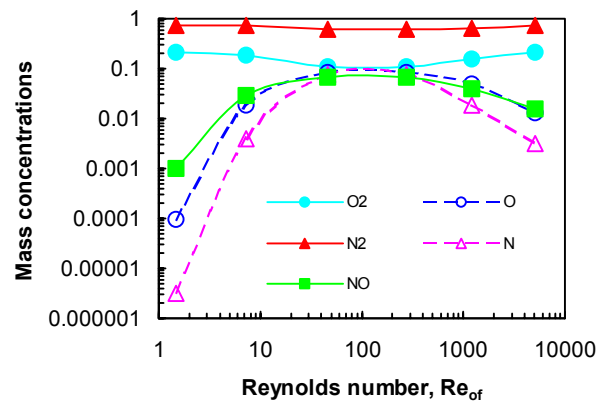

Fig. 7 Mass concentrations α_i of the dissociated air components on the external boundary of the TVSL as a function of the Reynolds number Re_{of}.

Figure 7 displays the distribution of the mass component concentrations α_i of the dissociating air [molecules of oxygen (filled circles), nitrogen (filled triangles), and nitric oxide (squares), as well as atoms of oxygen (empty circles) and nitrogen (empty triangles)] on the external boundary of the thin viscous shock layer at the values of the Reynolds number $1.49 \leq Re_{of} \leq 5130$. The data indicates that the catalytically active surface influences the full width of the viscous shock layer at the

Fig 6. Mass concentrations α_i of the air components in the TVSL at $Re_{of} = 230$: dash lines - ideally catalytic surface; solid lines - absolutely noncatalytic surface.

flight altitudes above 85 km. In the range of considered models of the TVSL under the terms of decreasing altitude (or the increase of the Reynolds number Re_{of}), concentration α_i on the external boundary of the layer reaches its value in upstream equilibrium flow [13, 14]. Under the conditions corresponding to the flight at the altitudes H $\leq$ 60 km, instead of modified conditions of Rankine-Hugoniot, it is possible, with acceptable accuracy, to use standard boundary conditions [9] at the shock wave.
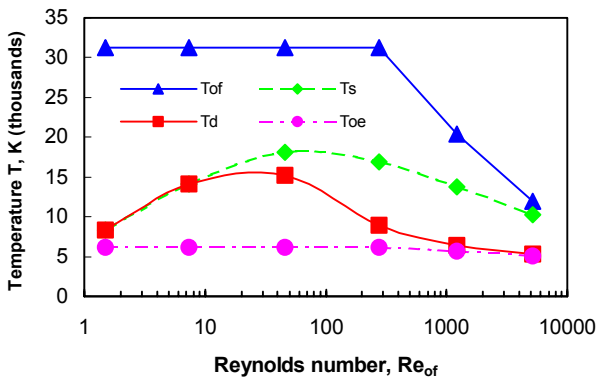

Fig. 8 The values of temperatures T_s, T_d, T_{of}, and T_{oe} as functions of Reynolds number Re_{of}.

The distributions of the temperature values T_s along the external boundary of TVSL (diamonds) and the stagnation temperature values T_{of} (triangles) are shown in Fig. 8. The distribution of T_s has a number of specific features in the different sections of the flight trajectory. As the Reynolds number Re_{of} increases, T_s rises at the range of altitudes from 110 to 90 km. As the altitude falls to 80 km, a relative stabilization of T_s occurs. Then a monotonous decrease of T_s is observed. This phenomenon is due to significant braking [17] of the vehicle in layers of high-density atmosphere and to decrease of T_{of} (see Fig. 8). In the case of relatively large values of Reynolds number $Re_{of} \geq$ 230, the regular boundary layer begins to be formed inside the TVSL. The width of the catalytically influenced zone d is its specific characteristic (see Fig. 6). We have used the distribution of the mass concentration of oxygen atoms for the determination of d because of the significant sensitivity of the atoms to the catalysis at the vehicle surface. The other correlations of the

parameter d could be made if the other species are taken into consideration. The difference between the species distributions (see Fig. 6) and the corresponding parameters d can be explained by different transport properties of the air components [28].
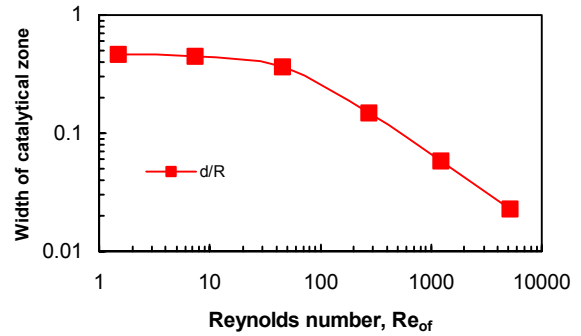

Fig. 9 The width of the catalytically influenced zone d as a function of Reynolds number Re_{of}.

As presented in Fig. 9, the results of calculations show that the value d correlates with the parameter Re_{of} according to the exponential law in the broad range of the Reynolds number $230 \leq Re_{of} \leq 5130$ and under the flight conditions at altitudes from 90 to 60 km. The distribution of the gas temperature value T_d (filled squares) on the conditionally introduced boundary d is shown in Fig. 8. As the altitude falls (from 90 km), a significant decrease of temperature T_d is observed on the assumed boundary of the catalytically influenced zone and the values T_d merge with the values [13] of the stagnation temperature T_{oe} corresponding to the equilibrium dissociated air state behind the shock wave (see Fig. 8, circles).
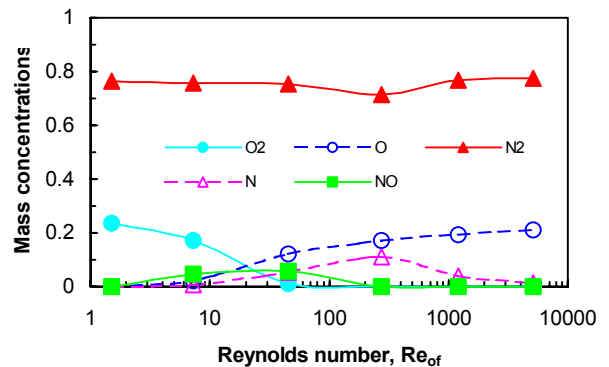

Fig. 10 Mass concentrations α_{iw} of air components on the noncatalytic vehicle surface.

Decrease of typical temperature in the TVSL with the decreasing flight altitude leads to the significant redistribution of the component concentrations (see Fig. 6). As a matter of fact, this phenomenon appears in the distribution of air species concentrations on the noncatalytic surface according to the changing flight altitude conditions. These correlations are shown in Fig. 10. The above-mentioned results point to the critical character of the flow at the altitude $h = 80$ km. The process of dissociation of molecules of oxygen and nitrogen is fully completed at this altitude. As a result, there is maximum presence of oxygen and nitrogen atoms.

Consequently, there was conducted an additional analysis of the characteristics of the flow in the TVSL at the altitude of 80 km. In particular, the influence of different models of evaluating the diffusion fluxes was studied. It appears that if thermodiffusion is considered, it leads to minor adjustments (no more than 2%) of the heat flux value and of distribution of species concentration values (about 4%). In the case of the absolutely noncatalytic surface, it is noticed, that using the approximation method [14, 28] of diffusion description (e.g., the Fick law at Schmidt numbers $Sc_i = 0.5$) leads to inaccuracies in the values of diffusion fluxes (up to 25%).

Moss [7], Miner and Lewis [8], Gusev et al. [10], Provotorov and Riabov [11-14], Schexnayder and Evans [38], and Blottner [39] used different expressions of the rates of chemical reactions as functions of temperature. The influence of this factor on the characteristics of thermal and mass transfer in the viscous shock layer may turn out to be very significant [14]. The following data confirms this statement. The value of the heat-transfer coefficient $C_h = 2q/(\rho_\infty U_\infty^3)$ obtained while using the constants [11] of chemical reactions considering the reaction $O_2 + N_2 = 2NO$, turns to be 0.04305. While using the constants [38] without considering the reaction, the value C_h is 0.03804. If the above reaction [38] is taken into consideration the heat transfer coefficient becomes 0.03806. While the value based on the reaction rates by Blottner [39] is 0.03685. Using

the reaction constants from Ref. 38 leads to the decrease of the heat flux towards the absolutely noncatalytic wall by 12% at the altitude of 80 km, but the constants recommended by Blottner [39] leads to the decrease of C_h by 14%. The greatest difference in the values of backward reaction constants, which are considered as functions of temperature, occurs in the dissociation-recombination reactions with participation of atoms of oxygen and nitrogen. The role of exchange reaction $O_2 + N_2 = 2NO$ is insignificant. In the case of ideally catalytic surface the usage of other values of the chemical reaction rates as the functions of temperature leads to minor changes (about 1-2%) in the values of the heat flux C_h or the Stanton number St [14].

This analysis demonstrates that in order to increase the accuracy of the determination of the heat flux characteristics in nonequilibrium viscous shock layer, it is recommended to use more reliable information on transfer properties [28] of multicomponent gas mixture and the constants [4] of chemical reaction rates. It is also found that the binary similitude law [10] is satisfied in all the researched conditions of streaming of blunt bodies.

4 Equilibrium temperature of the vehicle surface

Large values of the heat flux towards the surface of the spherical body under flight conditions at high altitudes lead to high level of equilibrium surface temperature $T_{we} = (q/\varepsilon\sigma)^{1/4}$, where ε is emissivity, and σ is the Stephan-Boltzmann's constant.
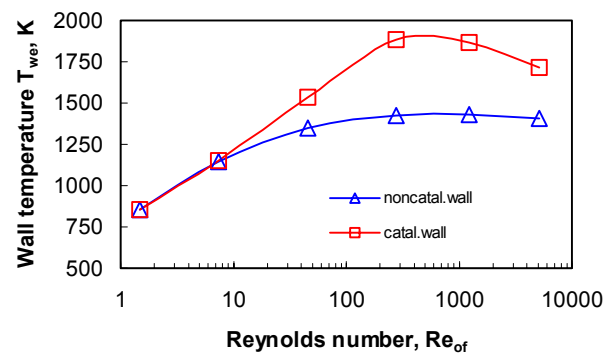

Fig. 11 Equilibrium temperature T_{we} of the spherical surface ($R = 1$ m) vs. Reynolds numbers Re_{of}.
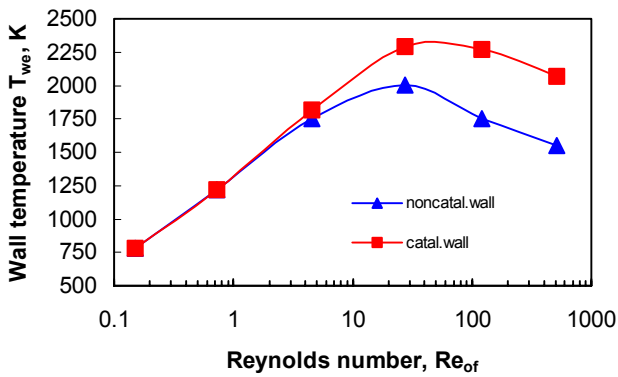
Fig. 12 Equilibrium temperature T_{we} of the cylindrical surface ($R = 0.1$ m) vs. Reynolds numbers Re_{of}.

In Figs. 11 and 12, as an example, the values T_{we} with $\varepsilon = 0.85$ are shown, for axisymmetrical critical point of the body with the blunt radius $R = 1$ m and on the critical line of a cylinder having $R = 0.1$ m for two extreme cases of catalytic activity of the vehicle surface. Using noncatalytic surface material (triangles) leads to a significant decrease in the equilibrium temperature.

Fig. 13 demonstrates the influence of the swept angle χ on the equilibrium temperature T_{we} along the critical line of the cylindrical surface ($R = 1$ m) for two extreme cases of the process of heterogeneous reactions (on three points of the trajectory [17, 24]): solid lines correspond to noncatalytic, and dashed lines - to the ideally catalytic wall of the vehicle.
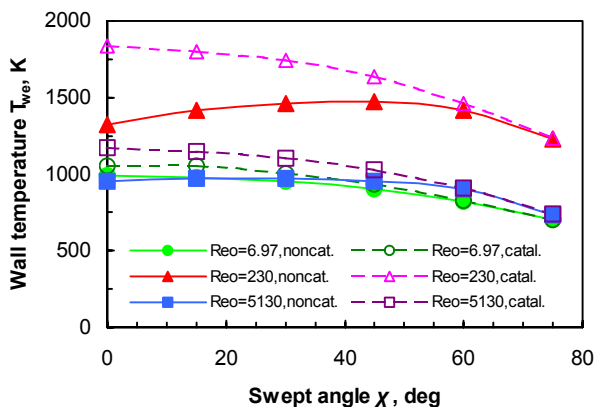

Fig. 13 Equilibrium temperature T_{we} of the cylindrical surface ($R = 1$ m) as a function of the swept angle χ for different values of the Reynolds number Re_{of}: solid lines - noncatalytic surface; dashed lines - catalytic surface.

The calculations indicate that the equilibrium temperature of the surface monotonously decreases as the angle increases and only slightly depends on the mechanism of the process of the reactions on the surface. The degree of the gas dissociation is significant under the conditions of maximum heat fluxes ($Re_{of} = 230$, $h = 80$ km), hence leading to the substantial difference of the value $T_{we}(\chi)$ for different materials of the surface [14]. As for the absolutely noncatalytic wall, this value carries nonmonotonous character, and in the point of maximum T_{we} the value of equilibrium temperature is approximately 150K higher then of the corresponding value when $\chi = 0$. As the further decrease of the altitude occurs, these differences decrease. The explanation of this effect is: as the swept angle gets bigger, the degree of dissociation of gas decreases in the viscous shock layer [40, 41]. This consequence leads to the decrease of the part of energy of the free upstream flow, which is directed towards the dissociation of the molecules and to the decrease of influence of noncatalytic surface on the heat flux. As a result, the equilibrium temperature T_{we} approaches the value that corresponds to the ideally catalytic surface.

Under considered flight conditions the pattern of the heat flux depending on the swept angle fully corresponds to the changes of the equilibrium temperature of the surface.

Conclusion

The considered computational tests were conducted specifically as a model problem for preliminary design of heat protection systems of hypersonic vehicles such as the Space Shuttle. The computed results presented in this study further validate the TVSL model for calculating nonequilibrium multicomponent gas flow near blunt bodies under rarefied-gas flight and wind-tunnel test conditions. The understanding of the main characteristics of the catalytically influenced zone can be useful for creation of new approximation methods of describing heat flux at a catalytic surface of a vehicle.

Acknowledgment

References

[1] Gnoffo P. Planetary-entry gas dynamics. *Annual Review of Fluid Mechanics*, Vol. 31, pp. 459-494, 1999.

[2] Cheng H. Perspectives on hypersonic viscous flow research. *Annual Review of Fluid Mechanics*, Vol. 25, pp. 455-484, 1993.

[3] Koppenwallner G. Fundamentals of hypersonics: aerodynamics and heat transfer. *Hypersonic Aerothermodynamics*, Deutsche Forschungs- und Versuchsanstalt fhr Luft- und Raumfahrt E. V., Lecture Series, No. 1984-01, DFVLR-Press, 1984.

[4] Park C, Howe J, Jaffe R and Candler G. Review of chemical-kinetic problems of future NASA missions, II: Mars entries. *Journal of Thermophysics and Heat Transfer*, Vol. 8, No. 1, pp. 9-23, 1994.

[5] Grumet A, Anderson J and Lewis M. Numerical study of the effects of wall catalysis on shock wave/boundary-layer interaction. *Journal of Thermophysics and Heat Transfer*, Vol. 8, No. 1, pp. 40-47, 1994.

[6] Cheng H. The blunt-body problem in hypersonic flow at low Reynolds number. Paper No. 63-92, IAS, New York, 1963.

[7] Moss J. Reacting viscous-shock-layer solutions with multicomponent diffusion and mass injection. NASA TR 411, Washington, DC, 1974.

[8] Miner H and Lewis C. Hypersonic ionizing air viscous shock-layer flows over nonanalytic blunt bodies. NASA CR 2550, Washington, DC, 1975.

[9] Anderson J. *Hypersonic and high temperature gas dynamics*, McGraw-Hill, New York, NY, 1989.

[10] Gusev V, Provotorov V and Riabov V. Effect of physical and chemical nonequilibrium on simulation of hypersonic rarefied gas flows. *Fluid Mechanics - Soviet Research*, Vol. 10, No. 5, pp. 123-135, 1981.

[11] Provotorov V and Riabov V. Study of nonequilibrium hypersonic viscous shock layer. *Trudy TsAGI*, Issue 2111, pp. 142-156, 1981 (in Russian).

[12] Provotorov V and Riabov V. Study of hypersonic flows in a thin viscous shock layer in the presence of nonequilibrium dissociation and ionization. *Uchenyye Zapiski TsAGI*, Vol. 12, No. 5, pp. 55-63, 1981 (in Russian).

[13] Provotorov V and Riabov V. Effect of chemical reactions on the flow of air in a viscous shock layer. *Fluid Mechanics - Soviet Research*, Vol. 12, No. 6, pp. 17-25, 1983.

[14] Provotorov V and Riabov V. Investigation of a structure of a multicomponent viscous shock layer. *Trudy TsAGI*, Issue 2436, pp. 152-164, 1990 (in Russian).

[15] Riabov V and Provotorov V. The structure of multicomponent nonequilibrium viscous shock layers. AIAA Paper, No. 94-2054, 1994.

[16] Botin A, Gusev V, Provotorov V, Riabov V and Chernikova L. Study of the influence of physical processes on heat transfer toward the blunt bodies in flows with small Reynolds numbers. *Trudy TsAGI*, Issue 2436, pp. 134-144, 1990 (in Russian).

[17] Tong H, Buckingham A and Curry D. Computational procedure for evaluations of Space Shuttle TRS requirements. AIAA Paper 74-518, 1974.

[18] Gupta R, Lee K, Zoby E and Thompson R. Hypersonic viscous shock-layer solutions over long slender bodies - Parts I-II. *Journal of Spacecraft and Rockets*, Vol. 27, No. 2, pp. 175-193, 1990.

[19] Gupta R, Nayaui S, Lee K and Zoby E. High-order viscous shock-layer solutions for high altitude flows. AIAA Paper 93-2724, 1993.

[20] Gupta R, Yos J, Thompson R and Lee K. A review of reaction rates and thermodynamic and transport properties for an 11-species air model for chemical and thermal nonequilibrium calculations to 30,000K. NASA Reference Publication No. 1232, 1990.

[21] Gupta R and Simmonds A. Hypersonic low-density solutions of the Navier-Stokes equations with chemical nonequilibrium and multicomponent surface slip. AIAA Paper 86-1349, 1986.

[22] Jain A and Prabha S. A comparative study of stagnation-point hypersonic viscous shock-layer and hypersonic merged-layer flows. *Proc. 14th International Symposium on Rarefied Gas Dynamics*, edited by Hakuro Oguchi, University of Tokyo, Vol. I, pp. 241-248, 1984.

[23] Molodtsov V and Riabov V. Investigation of the structural features of rarefied gas flows about a sphere using Navier-Stokes equations. *Proc. 13th International Symposium on Rarefied Gas Dynamics*, Novosibirsk, Vol. 1, pp. 535-541, 1985.

[24] Moss J and Bird G. Direct simulation of transitional flow for hypersonic reentry conditions. AIAA Paper No. 84-0223, 1984.

[25] Bird G. *The DS2G Program User's Guide, Version 2.3*. Killara, Australia, 1999.

[26] Riabov V. Heat transfer on a hypersonic sphere with diffuse rarefied-gas injection. AIAA Paper 2004-1176, 2004.

[27] Riabov V and Botin A. Hypersonic hydrogen combustion in the thin viscous shock layer. *Journal of Thermophysics and Heat Transfer*, Vol. 9, No. 2, pp. 233-239, 1995.

[28] Riabov V. Approximate calculation of transport coefficients of Earth and Mars atmospheric dissociating gases. *Journal of Thermophysics and Heat Transfer*, Vol. 10, No. 2, pp. 209-216, 1996.

[29] Keller H. Accurate difference methods for nonlinear two-point boundary value problems. *SIAM Journal of Numerical Analysis*, Vol. 11, No. 2, pp. 305-320, 1974.

[30] Riabov V and Provotorov V. Exponential box-schemes for boundary-layer flows with blowing. *Journal of Thermophysics and Heat Transfer*, Vol. 10, No. 1, pp. 126-130, 1996.

[31] Nomura S. On a determination of heat flux at a critical stagnation point of a blunt body in hypersonic flow at small Reynolds numbers. *AIAA Journal*, Vol. 22, No. 7, 1984.

[32] Gusev V and Nikolsliy Yu. Experimental study of heat transfer at a critical stagnation point of a sphere in hypersonic rarefied-gas flow. *Uchenyye Zapiski TsAGI*, Vol. 2, No. 1, 1971 (in Russian).

[33] Klimova T and Chernikova L. A study of heat transfer in hypersonic rarefied-gas flow. *Rarefied Gas Dynamics. Proc. 6th All-Union Conference on RFG*. Novosibirsk, 1980 (in Russian).

[34] Vasiliev A and Vorobiev A. A study of heat exchange on long cylinders at different angles of attack in supersonic rarefied-gas flow. *Rarefied Gas Aerodynamics*, No. 7, Leningrad State University, Leningrad, 1974 (in Russian).

[35] Zavarzina I, Vasiliev A and Prokopenko N. A study of local heat exchange on infinitely long cylinders in supersonic rarefied-gas flow. *Rarefied Gas Dynamics. Proc. 3rd All-Union Conference on RFG*. Novosibirsk, 1971 (in Russian).

[36] Botin A. A Study of local heat transfer to the spherical surface with gas injection at small Reynolds numbers. *Uchenyye Zapiski TsAGI*, Vol. 18, No. 5, pp. 41-47, 1987 (in Russian).

[37] Throckmorton D. Benchmark Aeroheating data from the first flights of the Space Shuttle Orbiter. AIAA Paper, No. 82-0003, 1982.

[38] Schexnayder C and Evans J. Influence of ablation impurities on blunt re-entry ionizations. *AIAA Journal*, Vol. 12, No. 6, pp. 805-811, 1974.

[39] Blottner F. Nonequilibrium laminar boundary layer flow of ionized air. *AIAA Journal*, Vol. 2, No. 11, pp. 1921-1927, 1964.

[40] Gershbein E, Peigin S and Tirskiy G. Supersonic flow around bodies at low and moderate Reynolds numbers. *Itogi Nauki i Tekhniki. VINITI. Ser. Mech. Fluids & Gases*, Vol. 19, pp. 3-85, 1985 (in Russian).

[41] Gershbein E, Schelin V and Yunitskiy S. Hypersonic chemically nonequilibrium viscous shock layer on wings with catalytic surface. *Fluid Dynamics*, Vol. 19, No. 6, 1984.